Trophic transfer of silver nanoparticles shifts metabolism in snails and reduces food safety

Dang, F.; Li, C.; Nunes, L.M.; Tang, R.; Wang, J.; Dong, S.; ... ; Sonne, C.

Environment International 176 (2023) 107990

Contents lists available at ScienceDirect

Environment International

journal homepage: www.elsevier.com/locate/envint

Full length article

Trophic transfer of silver nanoparticles shifts metabolism in snails and reduces food safety

Fei Dang [a,b], Chengcheng Li [a,*], Luís M. Nunes [c], Ronggui Tang [a], Junsong Wang [d,*], Shuofei Dong [e], Willie J.G.M. Peijnenburg [f,g], Wenxiong Wang [h], Baoshan Xing [b], Su Shiung Lam [i,j], Christian Sonne [j,k,*]

[a] Key Laboratory of Soil Environment and Pollution Remediation, Institute of Soil Science, Chinese Academy of Sciences, Nanjing 210008, China
[b] Stockbridge School of Agriculture, University of Massachusetts, 161 Holdsworth Way, Amherst, MA 01003, United States
[c] University of Algarve, Civil Engineering Research and Innovation for Sustainability Center, Faro, Portugal
[d] Center for Molecular Metabolism, School of Environmental and Biological Engineering, Nanjing University of Science and Technology, Nanjing 210094, China
[e] Agilent Technologies Co. Ltd (China), No.3, Wang Jing Bei Road, Chao Yang District, Beijing 100102, China
[f] Institute of Environmental Sciences (CML), Leiden University, P.O. Box 9518, 2300 RA Leiden, the Netherlands
[g] National Institute of Public Health and the Environment (RIVM), P.O. Box 1, Bilthoven, the Netherlands
[h] School of Energy and Environment, City University of Hong Kong, Kowloon, Hong Kong
[i] Higher Institution Centre of Excellence (HICoE), Institute of Tropical Aquaculture and Fisheries (AKUATROP), Universiti Malaysia Terengganu, 21030 Kuala Nerus, Terengganu, Malaysia
[j] School of Forestry, Henan Agricultural University, Zhengzhou 450002, China
[k] Department of Ecoscience, Aarhus University, Frederiksborgvej 399, PO Box 358, DK-4000 Roskilde, Denmark

ARTICLE INFO

Handling Editor: Adrian Covaci

Keywords:
Nano-agriculture
Biomagnification
Metabolism
Human health
Food safety

ABSTRACT

Food security and sustainable development of agriculture has been a key challenge for decades. To support this, nanotechnology in the agricultural sectors increases productivity and food security, while leaving complex environmental negative impacts including pollution of the human food chains by nanoparticles. Here we model the effects of silver nanoparticles (Ag-NPs) in a food chain consisting of soil-grown lettuce *Lactuca sativa* and snail *Achatina fulica*. Soil-grown lettuce were exposed to sulfurized Ag-NPs via root or metallic Ag-NPs via leaves before fed to snails. We discover an important biomagnification of silver in snails sourced from plant root uptake, with trophic transfer factors of 2.0–5.9 in soft tissues. NPs shifts from original size (55–68 nm) toward much smaller size (17–26 nm) in snails. Trophic transfer of Ag-NPs reprograms the global metabolic profile by down-regulating or up-regulating metabolites for up to 0.25- or 4.20- fold, respectively, relative to the control. These metabolites control osmoregulation, phospholipid, energy, and amino acid metabolism in snails, reflecting molecular pathways of biomagnification and pontential adverse biological effects on lower trophic levels. Consumption of these Ag-NP contaminated snails causes non-carcinogenic effects on human health. Global public health risks decrease by 72% under foliar Ag-NP application in agriculture or through a reduction in the consumption of snails sourced from root application. The latter strategy is at the expense of domestic economic losses in food security of $177.3 and $58.3 million annually for countries such as Nigeria and Cameroon. Foliar Ag-NP application in nano-agriculture has lower hazard quotient risks on public health than root application to ensure global food safety, as brought forward by the United Nations Sustainable Development Goals.

1. Introduction

Nearly 2 billion people suffer from *hidden hunger* micronutrient deficiencies while 795 million people face malnutrition worldwide (Food and Agriculture Organization of the United Nations, 2019). Extreme climate events and the coronavirus disease (COVID-19) pandemic exacerbate the threats to global food security (Hasegawa et al., 2021; Laborde et al., 2021). As such, sustainable agricultural development is of global concern and a priority of national and global organizations. This is illustrated in the Sustainable Development Goals (SDGs) of United

* Corresponding authors at: Department of Ecoscience, Aarhus University, Frederiksborgvej 399, PO Box 358, DK-4000 Roskilde, Denmark
E-mail addresses: ccliissas@163.com (C. Li), wang.junsong@gmail.com (J. Wang), cs@ecos.au.dk (C. Sonne).

https://doi.org/10.1016/j.envint.2023.107990
Received 9 January 2023; Received in revised form 14 April 2023; Accepted 21 May 2023
Available online 25 May 2023

Nations, including food security and sustainable agriculture (#2), sustainable consumption and production patterns (#12) and sustainable use of terrestrial ecosystems (#15) (United Nations, 2015). Nanotechnology makes substantial contributions in agricultural sustainability. For example, NPs increase nutrient-use efficiency, target specific plant tissues or pests, and improve soil structure and health (Hofmann et al., 2020; Wang et al., 2020; White and Gardea-Torresdey, 2018). However, it also has spurred both public and regulatory concerns due to potential adverse environmental and human health effects (Gilbertson et al., 2020; Lombi et al., 2019). Notably, because of direct and indirect interactions of nanoparticles (NPs) with target and non-target organisms, including plants, pests and humans, in the complex agricultural systems, we far from understand the environmental safety and human health risks of intentional NP application in agricultural practices (Dang et al., 2021; Hofmann et al., 2020; Pang et al., 2017). There is an urgent need to address this barrier to achieve true win–win solutions, in which improvement of agricultural production, enhancement of environmental sustainability and minimization of negative human health can be achieved synergistically (Lowry et al., 2019).

NPs undergo numerous and dynamic physical, chemical and biological transformation in soils and plants. These transformations may alter the original particle properties designed for specific function, leading to different bioavailability and toxicity in food chains (Dang et al., 2021). For example, antifungal and bactericidal NPs such as silver-based NPs (Ag-NPs) are estimated to be 0.1–2.2 ng kg^{-1} in soils, but tend to increase upon nano-agriculture practices (Hauser and Nowack, 2021). They sulfurize in soil and rhizosphere, resulting in metallic Ag-NPs entering the terrestrial food chains via plant leaves and sulfurized Ag-NPs in plant root (Larue et al., 2014; Pradas del Real et al., 2016; Stegemeier et al., 2015). Root uptake of silver sulfide NPs is more feasible for trophic transfer to herbivores relative to foliar uptake of metallic Ag-NPs (Dang et al., 2019). Even for foliar exposure, NPs internalized by plant leaves exhibit greater bioavailability during trophic transfer than those adsorbed on the leaves (Judy et al., 2012; Ma et al., 2018). Moreover, hazardous effects of accumulated Ag-NPs in edible portions of plants are documented for non-target predators leading to locomotion inhibition of springtails and snail feeding (Kwak and An 2016; Wu et al., 2021). However, a cohesive understanding of the relevance of these phenotypical observations and underlying mechanisms of action remains unclear. The lack of knowledge, in turn, hampers the identification of biomarkers of non-target predators used as early warning systems of ecosystem services.

Here, we address a longstanding challenge of assessing trophic transfer and the associated unintended impacts after Ag-NP application in agriculture. We hypothesize that Ag-NP application routes (foliar vs. root application) and initial Ag species (Ag-NPs vs. Ag(I)) would be the drivers of NP impacts in a lettuce-snail food chain. We first evaluate how Ag-NPs transform during trophic transfer using single-particle inductively coupled plasma mass spectrometry. We then reveal unexpected effects on snails using high-throughput metabolome, and identify the most important driver(s) of Ag-NP metabolite distinctions. In particular, the systemic responses of snails to Ag-NP trophic transfer are compared with Ag(I). We further evaluate the impacts of Ag-NP accumulation in snails on global health and food security using Monte Carlo simulation. After examining human hazard quotient risks from snail consumption, we find that foliar application of Ag-NPs is a better practice than root application in nano-agriculture to minimize hazard quotient risks and economic loss.

2. Material and methods

2.1. Nanoparticle characterization

Polyvinylpyrrolidone (PVP)-coated Ag-NPs, one of the most widely used metallic Ag-NPs, was purchased as powder from Emperor Nano Material Co., Ltd (Nanjing, China). NP suspensions (100 μg mL^{-1}, pH 6.0 ± 0.1) were prepared by dispersing the powder in ultrapure water followed by ultrasonication for 20 min prior to the experiments. The diameters and zeta potential of metallic Ag-NPs in ultrapure water were determined by transmission electron microscopy (JEOL JEM-2100, Japan) and Nano ZS (Zen 3600, Malvern, Australia), respectively.

2.2. Soil preparation

Surface sandy loam soil (0 – 20 cm depth) was collected from a pristine area in Yichang County, Hubei Province, China. A portion of air-dried soil without Ag addition was sieved through a 1.0-mm mesh and its physicochemical properties were characterized (Table S1). Other portions were sieved through a 4.0-mm mesh and spiked with Ag either in the form of metallic Ag-NP powder (500 and 1,000 μg g^{-1}) or $AgNO_3$ powder (50 μg g^{-1}). The spiked soil was thoroughly mixed, manually shaken, moistened with ultrapure water to 70% of the water holding capacity and aged in the dark at 25 °C. After aging for 28 days, the NPs in soil were directly examined using transmission electron microscopy and their elemental composition was determined using energy dispersive X-ray spectroscopy (TEM-EDS, Hitachi HT-7700, Japan) without NP isolation.

2.3. Lettuce exposure

Lettuce (*Lactuca sativa*) seeds were surface-sterilized with 1% NaClO for 30 min, and swelled in ultrapure water for 30 min. They were then germinated on a moistened filter in a petri dish in the dark at 18 ± 1 °C and 75% relative humidity for 2 weeks, followed by another 2 weeks in Hoagland solution in a climate chamber with a light: dark cycle of 16: 8 h at 20 ± 1 °C and 70% relative humidity. Afterwards, uniform seedlings were transferred to 24 pots (20-cm diameter × 15-cm height, each filled with 1.5 kg soil) for 7-d exposure in eight different ways: Ag-NP accumulation via foliar or root uptake (4 groups, Foliar/NP_{low}, Foliar/NP_{high}, Root/NP_{low}, and Root/NP_{high}), Ag(I) accumulation via foliar or root uptake (2 groups, Foliar/Ag(I) and Root/Ag(I)) and the control (2 groups, Foliar/Control and Root/Control). The experimental design and exposure doses of all the treatments are provided in Table S2. Each treatment was replicated in triplicate.

For foliar uptake, lettuce was grown in Ag-free soil and carefully sprayed four times per day with a total of 100 mL of freshly prepared PVP-coated metallic Ag-NP suspension (1 or 10 μg mL^{-1}) or $AgNO_3$ (0.1 μg mL^{-1}) using acid-washed aerosol sprayers. Silver concentrations were comparable to these used for plant pathogens (Kim et al. 2008). The pots were covered with aluminum foil to avoid soil contamination during foliar spraying and separated from each other to avoid cross-contamination. As for root uptake, lettuce was exposed to Ag-NPs (500 or 1,000 μg g^{-1}) or $AgNO_3$ (50 μg g^{-1}). Because Ag-NPs exhibited greater phytoavailability via foliar exposure than root exposure (Li et al., 2017), high concentrations of Ag-NPs were used in soils to ensure similar silver accumulation in lettuce between exposure pathways. Silver concentrations were in the range of those typically used to assess the fate and toxicity of Ag-NPs (Cox et al., 2016) and those in the biosolids (Ma et al., 2014; Wang et al., 2018), but likely much higher than those expected in soils (Hauser and Nowack, 2021).

After 7-day exposure, the lettuce leaves were harvested, washed sequentially with flowing ultrapure water, 10 mM of HNO_3 and 10 mM of freshly prepared L-cysteine and finally with ultrapure water to remove the loosely bound Ag-NPs/Ag(I) (Li et al., 2020). This washing method removed 82.6 ± 2.2% of the total Ag from the leaf surfaces. The subsamples were frozen-dried for total Ag analysis, and the fresh leaves were fed to snails.

2.4. Trophic transfer

The snails (*Achatina fulica*) originated from a farm in Zhejiang

Province, China and were acclimated for 2 weeks under laboratory-controlled conditions (25 °C, 16: 8 h light: dark, 85% relative humidity) before feeding on Ag-NP contaminated lettuce leaves. The trophic transfer experiment was designed as a 7-day exposure in which four groups of snails (*Achatina fulica*) were fed lettuce exposed to Ag-NPs via leaves or roots, two groups were fed lettuce exposed to Ag(I) via leaves or roots, and another two groups were fed Ag-free lettuce. Each group of snails was established with triplicate samples, and each triplicate consisted of four snails (10.9 ± 1.2 g). Lettuce leaves were cut into small sections of ca. 1 cm^2 to ensure homogeneous Ag levels and supplied *ad libitum*. Leaves was renewed every other day and the feces were removed daily.

On day 7, the snails were rinsed and depurated for > 48 h until Ag was undetectable in the feces. Snails were euthanized, dissected at 4 °C, and the tissues were stored at − 70 °C until further analysis. Tissues for histopathology and the Nuclear Magnetic Resonance (NMR) analysis were freshly prepared.

2.5. Total silver determination

Total Ag in plant and snail tissues was analyzed using inductively coupled plasma mass spectrometry (ICP-MS, NexION 300, PerkinElmer, USA). Before ICP-MS measurement, Ag-NPs and $AgNO_3$ suspensions were digested in a concentrated HNO_3 at a ratio of 1: 10 (v: v); freeze-dried biological tissues were digested in a 4: 1 (v: v) mixture of HNO_3 and H_2O_2, followed by microwave treatment for 90 min at 300 °C (Ethos one, Milestone, Italy). Certified reference materials of citrus leaf (GBW 10020, Chinese Academy of Geophysical Sciences, China) and lobster hepatopancreas (LUTS-1, National Research Council Canada) were concurrently digested. The total mass of Ag-NPs suspensions was monitored, and the recovery was 93 ± 3% after acid digestion. Silver recovery from the reference materials was 109 ± 7% and 93 ± 6%, respectively.

2.6. Size distribution of Ag-NPs within snails

To isolate Ag-NPs from the snail gastrointestine and foot, these tissues were digested using 20% tetramethylammonium hydroxide (TMAH) (Gray et al., 2013). Briefly, 0.5 g of tissue was homogenized mechanically at 4 °C (28,000 rpm, 360 W; Ningbo Scientz Biotechnology, Ltd.), digested with TMAH (20% v/v, 10 mL) at 30 °C for 12 h and then allowed to settle for 1 h. The supernatant was diluted with ultrapure water prior to single-particle ICP-MS analysis (spICP-MS, Agilent 7900, Agilent Technologies, USA). As no reference material, i.e., biota tissues with known particle size of Ag-NPs is available, spiked recovery experiments were performed. Commercial reference materials of PVP-coated metallic Ag-NPs (30 and 70 nm, Nanocomposix, USA) were spiked in snail tissues and digested concurrently. TMAH digestion did not influence the particle size distribution of NPs (Fig. S1). Size detection limit of spICP-MS is 15 nm. Operational parameters and detailed information on spICP-MS analysis are summarized in Table S3 and Supplementary Text S1.

2.7. Histopathology and ^1H NMR analysis

Snail hepatopancreas, kidney and gastrointestine tissues were processed for histological examination (Eclipse E600, Nikon, Japan). Simultaneously, snail hepatopancreas and kidney, which were targets for Ag-NPs and displayed similar Ag concentrations across treatments, were analyzed using ^1H NMR spectroscopy. The ^1H NMR spectra data were pre-processed using Bruker Topspin 3.0 software (Bruker GmbH, Karlsruhe, Germany). Metabolites were identified using Chenomx NMR Suit 7.7 (Chenomx Inc., Edmonton, Canada). Biological pathway analysis was performed using MetaboAnalyst 2.0. The impact value threshold calculated for pathway identification was 0.8. Biological networks coupling pathways of nano-specific metabolism are constructed using the metabolic database in Foliar/NP_{high} and Root/NP_{high} groups. Further information on histopathology, NMR-based metabolic data processing and the statistical analyses are available in the Supplementary Text S2-3.

2.8. Health risk assessment and sensitivity analysis

Hazard quotients (HQ) is used to evaluate non-carcinogenic effects associated with snail consumption. HQ is the ratio of daily intake of Ag (DI, μg kg^{-1} BW d^{-1}) and reference dose (R_fD, μg kg^{-1} BW d^{-1}) according to the method (USEPA, 2011). Daily intake of Ag from snail consumption is obtained as follows:

$$DI = \frac{C \times CR}{BW} \quad (1)$$

Where C is silver concentration in snails (μg g^{-1}); CR is per capita consumption rate of snails (g d^{-1}), which is collected either from a questionnaire survey or literature (Supplementary Text S4); BW is body weight (kg). These parameters are listed in Table S4.

Monte Carlo Simulations (MCS) was used to assess uncertainty and model sensitivity quantitatively (Burmaster and Wilson, 1996; EFSA, 2012). Probability distributions were estimated from data sourced from published data. Sensitivity analysis was performed to identify the relative contribution of each variable to the total variance of the estimated hazard (HQs).

2.9. Economic loss of hazardous Ag-NP exposure

Economic impacts associated with hazardous Ag-NP exposure in snails under root application scenario were assessed according to those reported previously (Wu, 2007). We only estimated the economic losses in the marketplace, while the costs of implementing the regulative procedures was not considered.

The calculation of economic losses in trade (ELT) assumes that countries will apply the food safety regulations to protect the entire population from Ag-NP exposure at a hazard level (Mitchell, 2003), i.e., HQ ≥ 1. The probability p_i = P(HQ) ≥ 1 was computed by running Monte Carlo simulations on the hazard model and computing the *p* from the posterior distribution.

Economic losses in international trade and in the domestic markets are estimated by equations (2) and (3), respectively. Equation (2) followed closely the proposal proposed by Wu (2004), and was endorsed by the International Agency for Research on Cancer (IARC 2012), where (p_i) quantifies the reduced fraction in the imports per country.

$$ELT = Snail\ imports_i \times p_i \quad (2)$$

Where $Snail\ imports_i$ is measured in monetary units ($) for each individual country i.

Economic losses in the domestic market (ELD_i) is given by:

$$ELD_i = CR_i \times \beta_i \times \theta_i \times \rho_i \times \phi \times p_i \quad (3)$$

Where *CR* is per capita consumption rate in kg $year^{-1}$; β_i is population size (inhabitants), θ_i is the fraction of the total adult population that eat snails, ρ_i is the fraction of adults in the population, Φ_i is domestic market price of the snails ($ kg^{-1}).

3. Results and discussion

3.1. Ag-NP biotransformation and biomagnification

Metallic Ag-NPs had a TEM diameter of 55 ± 1 nm (Fig. 1A) and a zeta potential of −27.2 ± 3.2 mV in ultrapure water. After aging in the soil for 28 days, the TEM diameter of NPs increased to 68 ± 2 nm, and EDS analysis showed NPs contained silver and sulfur at a ratio of ca. 2:1 (Fig. 1B). Metallic Ag-NPs are sulfurized to silver sulfide via

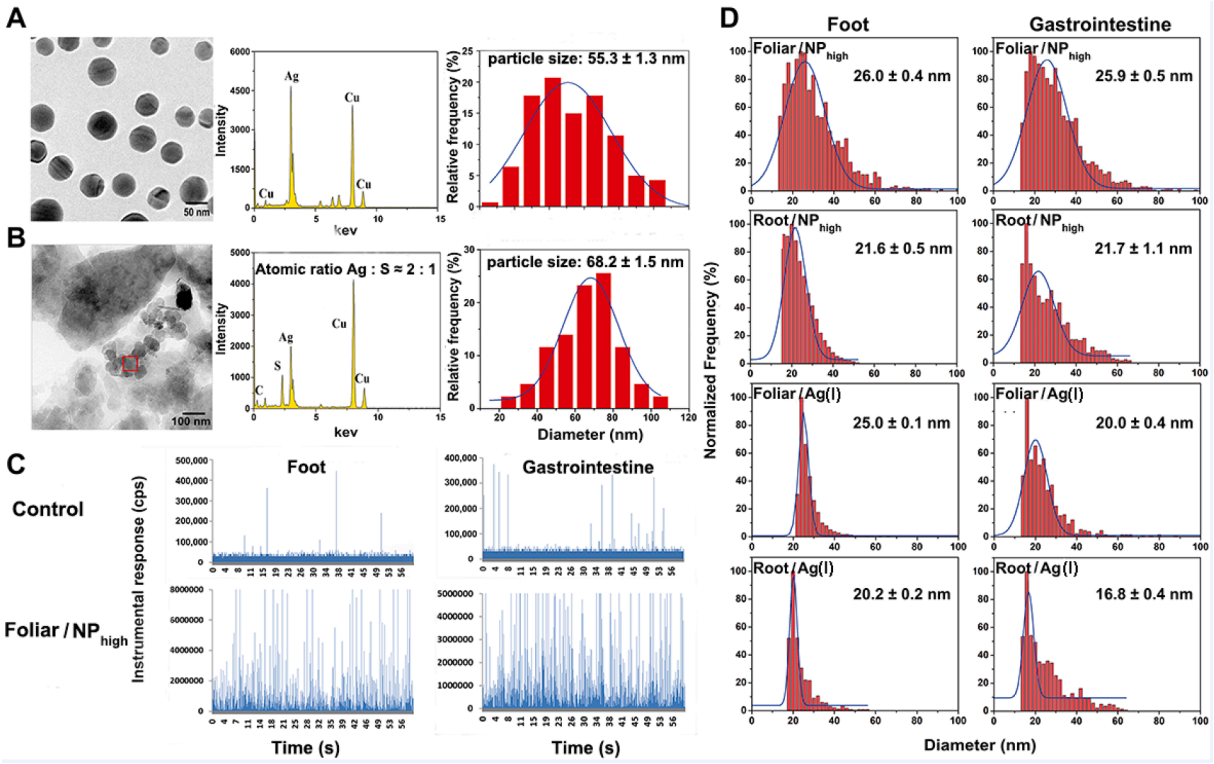

Fig. 1. Silver nanoparticle characterization. (A) Representative image of PVP-coated metallic Ag-NPs in ultrapure water for foliar application and their particle size distribution (n = 140) as measured by transmission electron microscopy-energy dispersive X-ray spectroscopy (TEM-EDS) analysis. The Cu peaks in the EDS spectra are due to Cu grid sample holder. (B) Representative image of NPs containing Ag and S in soil after 28-d aging and their particle size distribution (n = 43) as measured by TEM-EDS analysis. (C) Raw signal spectra of Ag-NPs in snail foot and gastrointestine from Foliar/NP_{high} group and the control group as measured by spICP-MS. (D) Histograms of particle size distribution of Ag-NPs in foot and gastrointestine of snails fed Ag-contaminated lettuce as measured by spICP-MS. NP_{high} and Ag(I) represent lettuce exposure to 10 and 0.1 μg Ag mL^{-1} upon foliar application, and to 1,000 and 50 μg Ag g^{-1} upon root application.

oxysulfidation reactions and/or via exchange and complexation reactions (He et al., 2019). Sulfidation of AgNPs capped by PVP occurs more difficult relative to those by citrate (Lieb et al., 2020; Liu et al., 2018).

Either foliar exposure to particulate Ag-NPs or root exposure to sulfurized Ag-NPs resulted in significant Ag accumulation in lettuce leaves and in snail tissues. Leaf Ag concentrations ranged from 1.5 ± 0.5 to 12.1 ± 5.8 μg g^{-1} (Fig. 2A). Most Ag in snails was distributed in the gastrointestine (22.6 – 99.3% of total Ag amount, averagely 12.0 μg g^{-1}), followed by the foot (0.08 – 74.7%, averagely 3.6 μg g^{-1}) > hepatopancreas (0.1 – 1.7%, averagely 0.07 μg g^{-1}) > kidney (0.03 – 1.7%, averagely 0.05 μg g^{-1}) (Fig. 2B-C, Fig. S2).

The size of Ag-NPs accumulating in snail foot and gastrointestine was smaller than that of the original applied ones (Fig. 1A-D). The appearance of smaller-sized Ag-NPs may result from the dissolution of original Ag-NPs, followed by Ag biotransformation into secondary particles (Laloux et al., 2020; Liu et al., 2022; Miclaus et al., 2016). Interestingly, Ag-NPs were also observed in the snails upon trophic transfer of Ag(I) (Fig. 1D), which again confirmed the Ag transformation *in planta* (Li et al., 2017), in the consumer (Liu et al., 2012; Okada et al., 2019), or

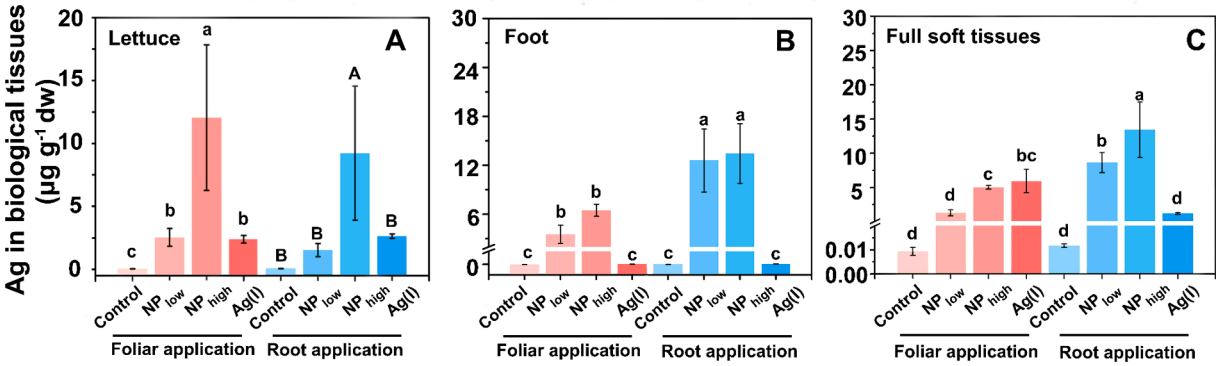

Fig. 2. Silver accumulation in lettuce leaves and snails. (A) Silver concentrations in the leaves of 35-d-old lettuce (the 3rd-5th leaves from lettuce apex) after 7 d exposure to Ag-NPs or Ag(I). NP_{low}, NP_{high} and Ag(I) represent lettuce exposure to 1, 10, and 0.1 μg Ag mL^{-1} upon foliar application, and to 500, 1,000, and 50 μg Ag g^{-1} upon root application. Lowercase and uppercase letters indicate significant differences within foliar or root application, respectively. Silver concentrations in (B) snail foot and (C) full soft tissues (i.e., foot and gastrointestine). Snails were fed Ag-contaminated lettuce for 7 d. Lowercase letters indicate significant differences in Ag concentrations ($P < 0.05$) across treatments, and uppercase letters indicate significant differences in TTFs ($P < 0.05$) across treatments. Data were analyzed using one-way ANOVA with LSD post hoc test. Data are the mean ± SD (n = 3).

both in conjunction. Where, how, and at what rates the transformation process occurs and whether surface coating of Ag-NPs (e.g., PVP or citrate) affects the transformation remains to be constrained. Similarly, *Daphnia magna* can dramatically modify the size distribution of Au-NPs from algae, and these nanoparticles, irrespective of initial size (10–100 nm), are of equivalent sizes in *D. magna* (28–38 nm), and remain almost the same in the intestine of fish as shown by spICP-MS analysis (Monikh et al., 2021). Biotransformation of NPs can benefit from techniques such as synchrotron-based X-ray microanalysis to identify the chemical speciation of the NPs and fluorescence to track intact particles. For instance, XANES analysis show that >85% of Ce(IV) is reduced to Ce(III) in digestive gland of snails consuming lettuce leaves via foliar exposure to CeO_2-NPs (Ma et al., 2018). In addition, the *in vivo* dissolution kinetics of algae-derived Ag-NPs are visualized in the gut of *Daphnia magna* using aggregation-induced emission fluorogen coated Ag-NPs (Yan and Wang, 2021). *Achatina fulica* is one of the most commonly consumed snails (Toader-Williams and Golubkina, 2009). Trophic transfer factors (TTFs) of Ag-NPs in snail foot and its full soft tissues (i.e., foot and gastrointestine) were at least 5 folds higher than those of Ag(I) (Fig. S3), highlighting the unique and high bioaccumulation of Ag-NPs. Furthermore, the calculated TTFs of Ag-NPs following root application were >1, indicating biomagnification through terrestrial food web (Fig. S3).

3.2. Global metabolome enables deeper biological understanding of Ag-NP trophic transfer

Trophic transfer has significant effects on snail's histopathology and global metabolic profile (Fig. 3). Hepatopancreas and kidney were targets for AgNPs, and displayed similar Ag concentrations between NP_{high} and Ag(I) groups, allowing for a direct comparison of the metabolic profiles (See Foliar/NP_{high} vs. Foliar/Ag(I) and Root/NP_{high} vs. Root/Ag (I) in Fig. S2). ^{1}H NMR spectroscopy of the hepatopancreas and kidney identified 28 and 38 metabolites, respectively (Fig. S4). After adjusting for confounding effects of shifts in the control, the univariate analysis further demonstrated considerable changes in hepatopancreas metabolites. These included 11 (7 up- and 4 down-regulated) in the Foliar/NP_{high} treatment; 6 (1 up- and 5 down-regulated) in the Root/NP_{high} treatment; 9 (all down-regulated) in the Foliar/Ag(I) treatment and 14 (11 up- and 3 down-regulated) in the Root/Ag(I) treatment (Fig. 3B). In the kidney, the total number of metabolites were 10 (5 up- and 5 down-regulated) in the Foliar/NP_{high} treatment; 14 (7 up- and 7 down-regulated) in the Root/NP_{high} treatment; 13 (4 up- and 9 down-regulated) in the Foliar/Ag(I) treatment; and 16 (10 up- and 6 down-regulated) in the Root/Ag(I) treatment (Fig. 3B). We mainly concentrate on metabolites in the hepatopancreas as the conclusions obtained from the hepatopancreas are also valid in the kidney.

The metabolites recognized from the global metabolome analysis of hepatopancreas differed between NP and Ag(I) groups (Fig. 3B). Although each application route led to comparable Ag burdens in the hepatopancreas between Ag(I) and NPs groups during trophic transfer (Foliar/NP_{high} vs. Foliar/Ag(I) and Root/NP_{high} vs. Root/Ag(I); Fig. S2), only few common metabolites such as succinate (down-regulated), glycine (down-regulated) and glucose (up-regulated) were shared, indicating shared common metabolic features between Ag(I) and NPs (Fig. 3B). Moreover, more metabolic variations were observed for NPs (e.g., putrescine, phosphocholine, N-acetylcyteine, maltose, lactate, glycine, glutamate, glucose, choline, betaine and alanine). Likewise, principal component analysis showed that the metabolites differed between Ag-NP and Ag(I) groups (Fig. 3C). These metabolite differences may reflect the complicated *in vivo* interaction of silver, derived from NPs- or Ag(I)- exposed lettuce, within biological systems. For example, biomolecular corona formation on Ag-NP surfaces may slow the

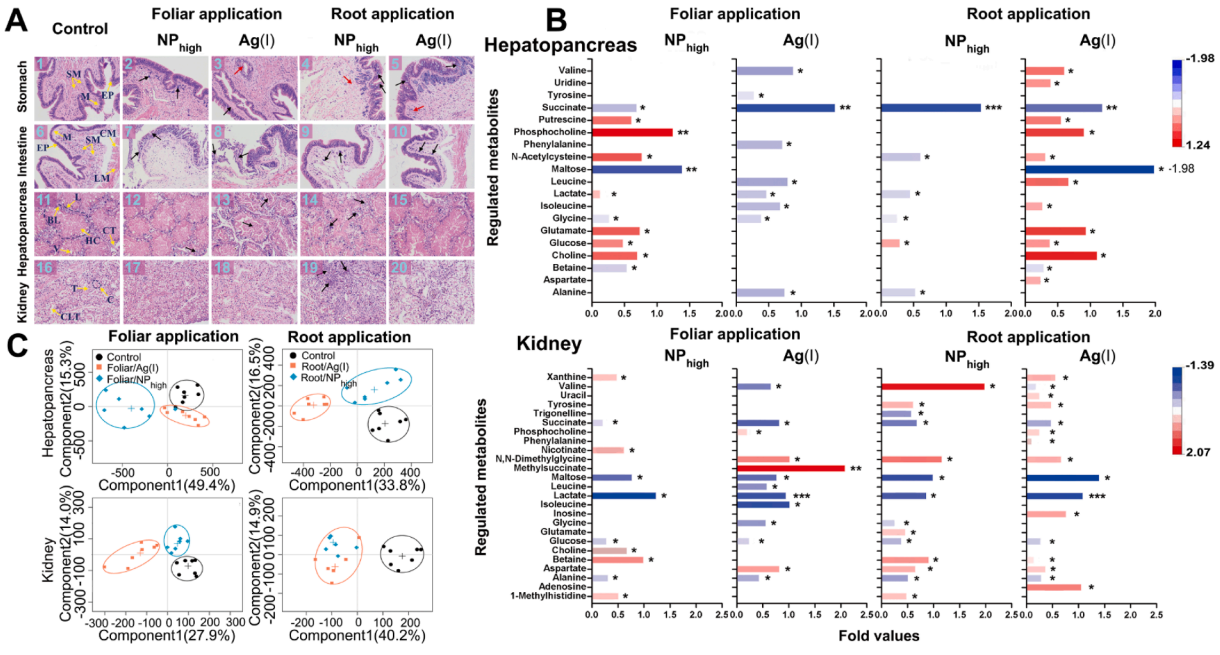

Fig. 3. Histological and metabolic responses of snails in responses to trophically available Ag. (A) Hematoxylin and eosin (H&E, ×200) analysis showed histological damages. In the control (images 1, 6, 11 and 16), epithelium (EP), submucosa (SM), mucosae (M), circular muscle (CM), longitudinal muscle (LM), lobule (L), connective tissues (CT), basal lamina (BL), hepatopancreas cells (HC), vacuoles (V), collecting tubule (CLT), corpuscle (C) and tubulointerstitium (T) are indicated by yellow arrows. Red arrows indicate cellular edema and partial abscess (image 3) and inflammatory edema of the submucosa (images 4 and 5). Black arrows indicate dilated and darkly stained nuclei (images 2, 9 and 10), cellular edema (image 3), abnormal goblet cells (images 4 and 5), erosions and ulceration of intestinal mucosal epithelial cells (images 7 and 8), pseudo-lobules and cell necrosis (images 12, 13 and 14) and interstitial fibrosis (image 19). (B) Significantly changed metabolites in exposed snails relative to the controls. The color codes (red: up-regulated; blue: down-regulated) indicate the $\log_2$ (fold) change. Significant differences were assessed using a parametric Student's *t*-test with a correction according to the Benjamini-Hochberg method. $^{*}P < 0.05$, $^{**}P < 0.01$, $^{***}P < 0.001$. (C) Scores of orthogonal signal correction-partial least squares-discriminant analysis (OSC-PLS-DA) of the metabolites across treatments. (For interpretation of the references to color in this figure legend, the reader is referred to the web version of this article.)

dissolution via promoting the sulfidation processes, and thus has potential implications for toxic effects (Miclaus et al., 2016). This illustrates the importance of evaluating the *in vivo* fate of silver to elucidate the distinct metabolite responses of trophically transferred Ag in nanoparticulate and ionic form. Nevertheless, the metabolism variations of NPs are partly from the released Ag(I) and partially due to their nanoscale physicochemical properties.

Fig. 4A summarizes the metabolic pathways upon Ag-NP trophic transfer. The consumption of lettuce exposed to Ag-NPs via either leaves or roots leads to a notable shift in snail energetic, osmoregulatory, phospholipid and amino acid metabolism. For example, the down-regulation of succinate implies the inhibition of the tricarboxylic acid (TCA) cycle, the central metabolic pathway linking the most metabolic pathways (e.g., glycolysis, gluconeogenesis, fatty acid metabolism and amino acid metabolism) (Horton et al., 1994). In parallel, the up-regulation of glucose indicates the compensation of cellular energy shortage via glycolysis to increase the adenosine trisphosphate (ATP) availability. Likewise, energy metabolism mode shifts from oxidative phosphorylation to glycolysis in tumor and non-tumor cells, upon direct exposure to metallic Ag-NPs (Chen et al., 2014). These metabolites shared by all Ag-NP groups support hazard identification of Ag-NP trophic transfer, allowing the identification of biomarkers for early detection of histopathology including cell membrane lesions and inflammation (Fig. 3A). Because the metabolome is dynamic, the extent to which these metabolites relate to histological outcome merits further investigation.

The metabolite profiles upon Ag-NP trophic transfer depend on the application route (Fig. 4A). The low conservation of responses across application routes highlights different modes of action of Ag-NPs during trophic transfer. For example, the up-regulation of glucose is coupled with the down-regulation of alanine, suggesting a Ag-NP-induced imbalance of the glucose-alanine cycle in snails consuming lettuce exposed to high level of Ag-NPs via root (Fig. 3B and Fig. 4A) (Sousa et al., 2016). However, up-regulation of glucose is associated with the breakdown of maltose in snails consuming lettuce exposed to high level of Ag-NPs through leaves (Fig. 3B and Fig. 4A). The low conservation of metabolic responses across application routes reflects the differences in Ag-NP transformation in the environment and food chain. For instance, metallic Ag-NPs are transformed as AgCl-NPs, Ag-glutathione or remain as metallic Ag-NPs within plants upon foliar application (Larue et al., 2014), while metallic Ag-NPs sulfurize in soils before plant uptake (Fig. 1B) (Li et al., 2020). Thus, those metabolites present exclusively in one application pathway allow limited extrapolation for other pathway. This illustrates the need to take the application routes of Ag-NPs at the entry of the food chain into account in agro-nanotechnology.

3.3. Driver of metabolic shift in snails

The observed molecular distinctions among treatments are the result of a combined effect of application routes and pristine Ag species (Ag-NPs or Ag(I)). In the hepatopancreas, this interaction was responsible for the overall variability in hepatopancreas (23%, $P = 0.001$) (Fig. 4B) and kidney (8.4%, $P = 0.03$) metabolites (Fig. 4C). Note that natural uncontrolled factors (e.g., biological variation among snails) (Smilde et al. 2005) dominated the overall variability in metabolites in the hepatopancreas (residuals > 73%, Fig. 4B) and in the kidney (residuals > 84%, Fig. 4C). The high proportion of metabolic backgrounds, therefore, should be taken into account in comparative environmental metabolome studies (Schweiger et al., 2014). Nevertheless, the ANOVA-ASCA analysis allowed a dissection of the combinatorial effect of metabolite backgrounds and designed environmental factors (i.e., pristine Ag species and plant uptake pathways), and revealed that the interaction of Ag species and plant uptake pathways imposes a stronger force in the metabolic features than does the single factor. Consequently, the failure to account for both the application routes and pristine Ag species in analysis of the trophic transfer of Ag-NPs leads to biased conclusions regarding the environmental impact of Ag-NPs.

3.4. Risks to global health and food security

A focus on the consequences of Ag-NP biomagnification following root application for global public health is of particular interest. Global snail trade provides a direct pathway studying Ag flows. Southern and Western Europe, Northern African countries, China and Republic of Korea represented over 99% of the total Ag flows (Fig. S7, Table S5). The largest Ag flow occurred between Spain and Morocco (15 – 153 kg Ag year^{-1}) with the latter being the largest European market supplier of snails. China is the main importing market of snails in Asia, and Ag was

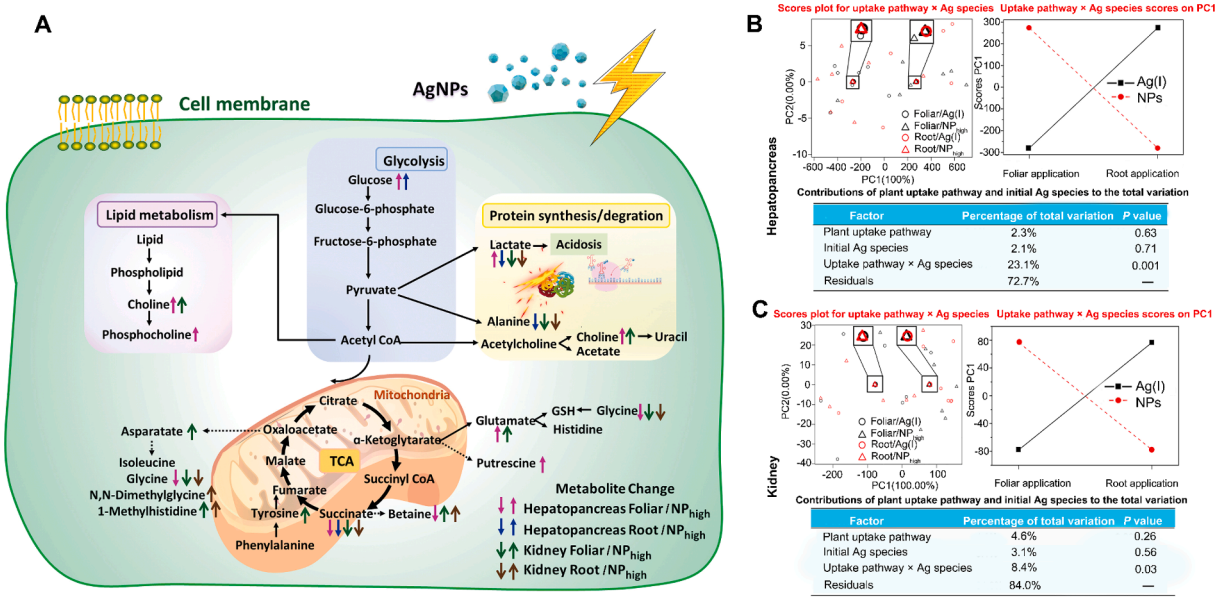

Fig. 4. (A) Schematic illustration of the global metabolic network in response to Ag-NP trophic transfer. Regulated metabolites (sourced from Fig. 3 and Fig. S4-S6) in snail hepatopancreas (red and blue) and kidney (green and brown) are shown in arrows. (B, C) ANOVA-simultaneous component analysis (ASCA) of the metabolic responses to trophically available Ag in (B) hepatopancreas and (C) kidney. (For interpretation of the references to color in this figure legend, the reader is referred to the web version of this article.)

mainly from Senegal (1.0 – 9.9 kg Ag year^{-1}), Republic of Korea (0.2 – 2.2 kg Ag year^{-1}), Canada (0.2 – 1.8 kg Ag year^{-1}) and Mauritania (0.2 – 1.6 kg Ag year^{-1}) (Table S5). In particular, the lowest Ag flow occurred in snails sourced from Foliar/NP_{low} lettuce among all Ag-NP groups.

We assessed the hazard quotients (HQ) of Ag-NPs, which reflect non-carcinogenic effects associated with snail intake. The HQ was the highest in Nigeria (>1 upon root application), where the per capita consumption rate was extraordinarily high (Fig. 5, Table S4). In contrast, the HQ for the populations with low (France and Italy) and medium (Spain, China, Portugal, and Cameroon) consumption rates are <1. For the most exposed individuals (90th percentile) within each population under root application scenario, HQ was above 1 in Cameroon and Nigeria, followed by Portugal, Spain and China (Table S6). This is raising a concern for human health risks caused by the global use of Ag-NP application in agricultural practices. Nevertheless, it is clear that the health risk of Ag-NPs under root application scenario is always higher than that under foliar application scenario. This is important since we approach the development of a sustainable nano-agriculture that balance costs and benefits while not affecting public health.

3.5. *Mitigation strategies for sustainable nano-agriculture*

To meet growing global snail demands and ensure food security while minimizing health risks, we consider two potential mitigation strategies. Central to these mitigation strategies was a recognition of the sensitivity of human health risks to Ag concentrations and consumption rates (Table S7). In the first scenario, nano-agriculture was restricted to foliar Ag-NP application and the Ag concentrations in snails decreased (Fig. 2C and Fig. S2). HQ in Nigeria was anticipated to drop by 72% (NP_{low}) and 52% (NP_{high}), respectively, as compared to the root application (Table S4). The second scenario was a reduction in the consumption of snails sourced from root application. For instance, consumption reduction under root application by 66% in Nigeria (i.e., from 24.70 to 8.40 g d^{-1}) decreased the HQ by 72% (refer the data for Nigeria and Cameroon in Table S4). This strategy would have almost the same reductions in HQ as in the first scenario for foliar Ag-NP application. Yet, the consumption reduction strategy had a large effect on domestic economic losses from domestic trade due to lower consumption rates, being $177.3 and $58.3 million per year for Nigeria and Cameroon, respectively (Table S8). The threat to silver biomagnification sourced from root application has profound consequences for losses in snail biomass for consumption. The impacts of Ag-NP at hazardous level (HQ $\geq$ 1) for Nigeria and Cameroon on international trade were minimal, because Nigeria repots no international trade of snails, while Cameroon has a loss of $1,700 per year (Table S8). Since the consumption reduction strategy has economical limits, foliar application strategy is the priority to minimize both environment and human impacts. This enables regulatory bodies to implement relevant safe guidelines on the use of silver nanoparticles in agricultural sectors.

4. Conclusion

This study provides evidence of food chain contamination by root application of Ag-NPs in nano-enabled agriculture that has unintended consequences for ecosystem services, adverse biological effects, food security and human health. Such effects are the result of a series of events, including silver biomagnification along the lettuce-snail food chain, metabolic shifts in snails and hazard quotient risks associated with snail consumption. We stress that although there are safety-related barriers to commercialization of nano-agrochemicals (Hofmann et al., 2020), these challenges could be surmounted by identifying potential nano-specific biomarkers and promising application approaches.

We discern the complex structure of metabolism to uncover the driver, which dictates the response of metabolic network to Ag-NP trophic transfer. We are currently at an early state of testing new biomarkers and long-term follow-up studies necessitate the identification of metabolites that relate to chronic ecosystem dysfunction. Adoption of these nanospecific biomarkers derived from metabolomics into routine assays could be a major step towards a risk-prevention-based paradigm to minimize unintentional consequences of Ag-NPs on ecosystem service. This also facilitates safe-by-design development of Ag-NPs and co-optimization of both safe and desired functionality of nano-agrochemicals and nanosensors in food (United Nations, 2015).

The results indicate that improper application approach of nano-agrochemicals (i.e., root application of Ag-NPs) may come with hazard quotient risks and thereby preventing nanotechnology from contributing significantly to global food security and safety and obstructing future sustainable development. Our scenarios suggest that, globally, foliar application of Ag-NPs has lower hazard quotient risks than root application on public health. Despite the data here represent lettuce production, a similar approach is applicable to other crops such as chili, radish, soybean and rice, in which foliar Ag-NP application is less phytotoxic and less accumulative in their edible portions, as compared to root application (Danget al., 2019; Li et al., 2017). Future research needs to consider all life-cycle stages of organisms to develop nanoagri-food techniques to minimize unintended consequences including shifts to non-target organisms (Avellan et al., 2021; Gilbertson et al., 2020).

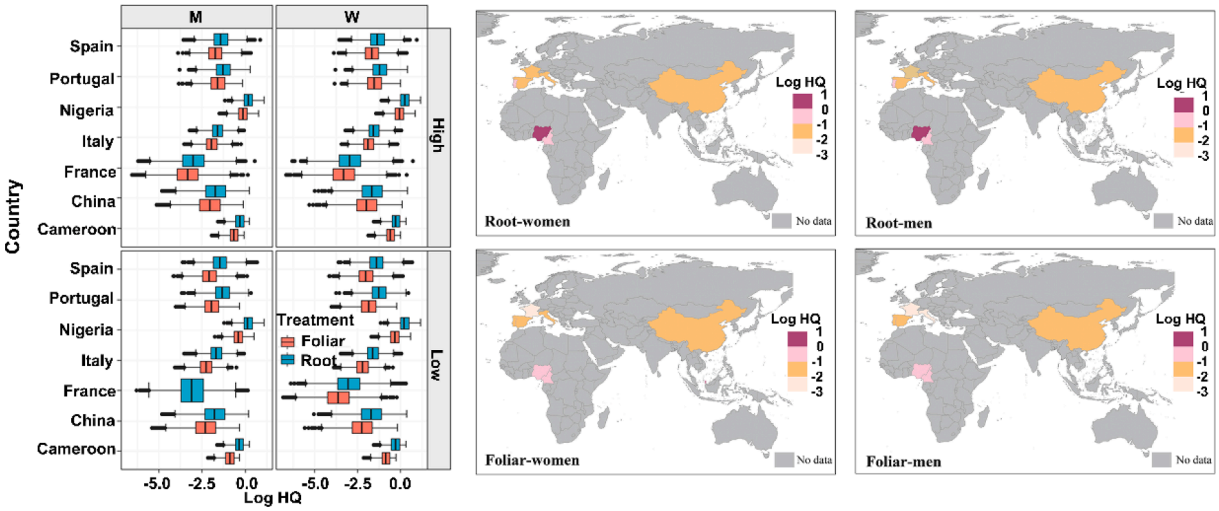

Fig. 5. Monte Carlo Simulation results for the hazard quotients (HQ) for human consumption of snails from Ag-NP groups at high and low levels. The color scales are in log-scale.

The systems-level trade-off analysis identify potential nanospecific biomarkers reflecting promising alternative for sustainable use of nano-agrochemicals. As more data become available, it enables a holistic and rigorous analysis of environmental trade-offs and further refines the opportunity space for the design and use of nano-enabled solutions. Our findings, together with the other barriers to the implementation of nano-agriculture technologies (Gilbertson et al., 2020; Hofmann et al., 2020) and consumer perceptions, highlight the importance of shifting towards sustainable nano-agriculture strategies to ensure global health and sustainability through the UN Sustainable Development Goals.

CRediT authorship contribution statement

Fei Dang: Conceptualization, Investigation, Project administration, Supervision, Writing – original draft, Writing – review & editing. **Chengcheng Li:** Methodology, Investigation, Project administration, Writing – original draft. **Luís M. Nunes:** Methodology, Writing – original draft. **Ronggui Tang:** Methodology. **Junsong Wang:** Methodology, Investigation, Writing – original draft. **Shuofei Dong:** Methodology. **Willie J.G.M. Peijnenburg:** Writing – review & editing. **Wenxiong Wang:** Writing – review & editing. **Baoshan Xing:** Writing – review & editing. **Su Shiung Lam:** Writing – review & editing. **Christian Sonne:** Writing – review & editing.

Declaration of Competing Interest

The authors declare that they have no known competing financial interests or personal relationships that could have appeared to influence the work reported in this paper.

Data availability

Data will be made available on request.

Acknowledgements

We thank the anonymous reviewers for their comments. We thank Minghui Li, from Nanjing University of Science and Technology, for the NMR analysis. We also thank the National Natural Science Foundation of China (41977355) for funding this research. Part of this study was supported by the Youth Innovation Promotion Association, CAS (20200314), and USDA-NIFA Hatch program (MAS00549). F.D. thanks the CSC for supporting her study at UMass Amherst for one year.

Appendix A. Supplementary data

Additional methods (Text S1-S4), including single particle inductively coupled plasma mass spectrometry Analysis, histological examination, metabolic data processing and statistical analysis, and survey of per capital consumption rate of snails; additional data (Fig. S1-S7, Table S1-S9), including Ag-NP characteristics, silver accumulation in snail tissues and trophic transfer factors, typical ^{1}H NMR spectra of metabolites in snail tissues, OSC-PLS-DA of the metabolic profiles from snail kidney and hepatopancreas, global trade flows of snails and silver, soil properties, experimental design for lettuce exposure, spICP-MS parameters, public hazard quotients, model sensitivity to input uncertainty of hazard quotients, economic loss associated with hazard Ag-NP exposure, and permuted P values for the ANOVA simultaneous component analysis, are provided in the Supporting Information. Supplementary data to this article can be found online at https://doi.org/10.1016/j.envint.2023.107990.

References

Avellan, A., Yun, J., Morais, B.P., Clement, E.T., Rodrigues, S.M., Lowry, G.V., 2021. Critical review: Role of inorganic nanoparticle properties on their foliar uptake and in planta translocation. Environ. Sci. Technol. 55 (20), 13417–13431.

Burmaster, D.E., Wilson, A.M., 1996. An introduction to second-order random variables in human health risk assessments. Hum. Ecol. Risk Assess. 2 (4), 892–919.

Chen, Y., Wang, Z., Xu, M., Wang, X., Liu, R., Liu, Q., Zhang, Z., Xia, T., Zhao, J., Jiang, G., Xu, Y., Liu, S., 2014. Nanosilver incurs an adaptive shunt of energy metabolism mode to glycolysis in tumor and nontumor cells. ACS Nano 8 (6), 5813–5825.

Cox, A., Venkatachalam, P., Sahi, S., Sharma, N., 2016. Silver and titanium dioxide nanoparticle toxicity in plants: A review of current research. Plant Physiol. Biochem. 107, 147–163.

Dang, F., Chen, Y.-Z., Huang, Y.-N., Hintelmann, H., Si, Y.-B., Zhou, D.-M., 2019. Discerning the sources of silver nanoparticle in a terrestrial food chain by stable isotope tracer technique. Environ. Sci. Technol. 53 (7), 3802–3810.

Dang, F., Huang, Y., Wang, Y., Zhou, D., Xing, B., 2021. Transfer and toxicity of silver nanoparticles in the food chain. Environ. Sci-Nano 8 (6), 1519–1535.

EFSA (European Food Safety Authority), 2012. Guidance on the use of probabilistic methodology for modelling dietary exposure to pesticide residues. EFSA Journal 10 (10), 2839.

FAO (Food and Agriculture Organization of the United Nations), 2019. The State of Food Security and Nutrition in the World. https://www.fao.org/3/ca5162en/ca5162en.pdf.

Gilbertson, L.M., Pourzahedi, L., Laughton, S., Gao, X., Zimmerman, J.B., Theis, T.L., Westerhoff, P., Lowry, G.V., 2020. Guiding the design space for nanotechnology to advance sustainable crop production. Nat. Nanotechnol. 15 (9), 801–810.

Gray, E.P., Coleman, J.G., Bednar, A.J., Kennedy, A.J., Ranville, J.F., Higgins, C.P., 2013. Extraction and analysis of silver and gold nanoparticles from biological tissues using single particle inductively coupled plasma mass spectrometry. Environ. Sci. Technol. 47 (24), 14315–14323.

Hasegawa, T., Sakurai, G., Fujimori, S., Takahashi, K., Hijioka, Y., Masui, T., 2021. Extreme climate events increase risk of global food insecurity and adaptation needs. Nat. Food 2, 587–595.

Hauser, M., Nowack, B., 2021. Probabilistic modelling of nanobiomaterial release from medical applications into the environment. Environ. Int. 146, 106184–106197.

He, D.i., Garg, S., Wang, Z., Li, L., Rong, H., Ma, X., Li, G., An, T., Waite, T.D., 2019. Silver sulfide nanoparticles in aqueous environments: formation, transformation and toxicity. Environ. Sci. Nano 6 (6), 1674–1687.

Hofmann, T., Lowry, G.V., Ghoshal, S., Tufenkji, N., Brambilla, D., Dutcher, J.R., Gilbertson, L.M., Giraldo, J.P., Kinsella, J.M., Landry, M.P., Lovell, W., Naccache, R., Paret, M., Pedersen, J.A., Unrine, J.M., White, J.C., Wilkinson, K.J., 2020. Technology readiness and overcoming barriers to sustainably implement nanotechnology-enabled plant agriculture. Nat. Food 1, 416–425.

Horton, H.R., Moran, A.L., Ochs, S.R., Rawan, J.D., Scrimgeour, K.G., 1994. Cell biochemistry and function. In: Patterson, N. (Ed.), Principles of biochemistry. John Wiley & Sons:, New York, p. 156.

IARC (International Agency for Research on Cancer), 2012. Economics of mycotoxins: evaluating costs to society and cost-effectiveness of interventions. IARC Sci. Publ. 158, 119–129.

Judy, J.D., Unrine, J.M., Rao, W., Bertsch, P.M., 2012. Bioaccumulation of gold nanomaterials by manduca sextathrough dietary uptake of surface contaminated plant tissue. Environ. Sci. Technol. 46 (22), 12672–12678.

Kim, H., Kang, H., Chu, G., Byun, H.S., 2008. Antifungal effectiveness of nanosilver colloid against rose powdery mildew in greenhouses. Solid State Phenom. 135, 15–18.

Kwak, J.I., An, Y.-J., 2016. Trophic transfer of silver nanoparticles from earthworms disrupts the locomotion of springtails (*Collembola*). J. Hazard. Mater. 315, 110–116.

Laborde, D., Herforth, A., Headey, D., de Pee, S., 2021. COVID-19 pandemic leads to greater depth of unaffordability of healthy and nutrient-adequate diets in low- and middle-income countries. Nat. Food 2, 473–475.

Laloux, L., Kastrati, D., Cambier, S., Gutleb, A.C., Schneider, Y.J., 2020. The food matrix and the gastrointestinal fluids alter the features of silver nanoparticles. Small 16, 1907687–1907698.

Larue, C., Castillo-Michel, H., Sobanska, S., Cécillon, L., Bureau, S., Barthès, V., Ouerdane, L., Carrière, M., Sarret, G., 2014. Foliar exposure of the crop *Lactuca sativa* to silver nanoparticles: Evidence for internalization and changes in Ag speciation. J. Hazard. Mater. 264, 98–106.

Li, C.-C., Dang, F., Li, M., Zhu, M., Zhong, H., Hintelmann, H., Zhou, D.-M., 2017. Effects of exposure pathways on the accumulation and phytotoxicity of silver nanoparticles in soybean and rice. Nanotoxicology 11 (5), 699–709.

Li, M., Liu, H.-L., Dang, F., Hintelmann, H., Yin, B., Zhou, D., 2020. Alteration of crop yield and quality of three vegetables upon exposure to silver nanoparticles in sludge-amended soil. ACS Sustain. Chem. Eng. 8 (6), 2472–2480.

Lieb, H.C., Nguyen, B.D., Ramsayer, E.R., Mullaugh, K.M., 2020. A voltammetric investigation of the sulfidation of silver nanoparticles by zinc sulfide. Sci. Total Environ. 720, 137685–137693.

Liu, N., Li, Y., Liu, L., Liu, X., Yin, Y., Qu, G., Shi, J., Song, M., Bin, H., Hu, L., Jiang, G., 2022. Administration of silver nasal spray leads to nanoparticle accumulation in rat brain tissues. Environ. Sci. Technol. 56, 403–413.

Liu, J., Wang, Z., Liu, F.D., Kane, A.B., Hurt, R.H., 2012. Chemical transformations of nanosilver in biological environments. ACS Nano 6 (11), 9887–9899.

Liu, J., Zhang, F., Allen, A.J., Johnston-Peck, A.C., Pettibone, J.M., 2018. Comparing sulfidation kinetics of silver nanoparticles in simulated media using direct and indirect measurement methods. Nanoscale 10 (47), 22270–22279.

Lombi, E., Donner, E., Dusinska, M., Wickson, F., 2019. A One Health approach to managing the applications and implications of nanotechnologies in agriculture. Nat. Nanotechnol. 14 (6), 523–531.
Lowry, G.V., Avellan, A., Gilbertson, L.M., 2019. Opportunities and challenges for nanotechnology in the agri-tech revolution. Nat. Nanotechnol. 14 (6), 517–522.
Ma, R., Levard, C., Judy, J.D., Unrine, J.M., Durenkamp, M., Martin, B., Jefferson, B., Lowry, G.V., 2014. Fate of zinc oxide and silver nanoparticles in a pilot wastewater treatment plant and in processed biosolids. Environ. Sci. Technol. 48 (1), 104–112.
Ma, Y., Yao, Y., Yang, J., He, X., Ding, Y., Zhang, P., Zhang, J., Wang, G., Xie, C., Luo, W., Zhang, J., Zheng, L., Chai, Z., Zhao, Y., Zhang, Z., 2018. Trophic transfer and transformation of CeO_2 nanoparticles along a terrestrial food chain: Influence of exposure routes. Environ. Sci. Technol. 52 (14), 7921–7927.
Miclaus, T., Beer, C., Chevallier, J., Scavenius, C., Bochenkov, V.E., Enghild, J.J., Sutherland, D.S., 2016. Dynamic protein coronas revealed as a modulator of silver nanoparticle sulphidation in vitro. Nat. Commun. 7, 11770–11780.
Mitchell, L., 2003. Economic theory and conceptual relationships between food safety and international trade. In: International Trade and Food Safety: Economic Theory and Case Studies. in: Agriculture U.S.D.O., ed. Washington, D.C., EUA. https://www.ers.usda.gov/webdocs/publications/41603/15636_aer828d_1_.pdf?v=0.
Monikh, F.A., Chupani, L., Arenas-Lago, D., Guo, Z.L., Zhang, P., Darbha, G.K., Valsami-Jones, E., Lynch, I., Vijver, M.G., van Bodegom, P.M., Peijnenburg, W., 2021. Particle number-based trophic transfer of gold nanomaterials in an aquatic food chain. Nat. Commun. 12, 899–911.
Okada, S., Chen, C., Watsuji, T.-o., Nishizawa, M., Suzuki, Y., Sano, Y., Bissessur, D., Deguchi, S., Takai, K., 2019. The making of natural iron sulfide nanoparticles in a hot vent snail. Proc. Natl. Acad. Sci. U.S.A. 116 (41), 20376–20381.
Pang, C., Hristozov, D., Zabeo, A., Pizzol, L., Tsang, M.P., Sayre, P., Marcomini, A., 2017. Probabilistic approach for assessing infants' health risks due to ingestion of nanoscale silver released from consumer products. Environ. Int. 99, 199–207.
Pradas del Real, A.E., Castillo-Michel, H., Kaegi, R., Sinnet, B., Magnin, V., Findling, N., Villanova, J., Carrière, M., Santaella, C., Fernández-Martínez, A., Levard, C., Sarret, G., 2016. Fate of Ag-NPs in sewage sludge after application on agricultural soils. Environ. Sci. Technol. 50 (4), 1759–1768.
Schweiger, R., Baier, M.C., Persicke, M., Muller, C., 2014. High specificity in plant leaf metabolic responses to arbuscular mycorrhiza. Nat. Commun. 5, 3886–3897.
Smilde, A.K., Jansen, J.J., Hoefsloot, H.C.J., Lamers, R.-J.- A.- N., van der Greef, J., Timmerman, M.E., 2005. ANOVA-simultaneous component analysis (ASCA): A new tool for analyzing designed metabolomics data. Bioinformatics (Oxford, England) 21 (13), 3043–3048.
Sousa, C.M., Biancur, D.E., Wang, X., Halbrook, C.J., Sherman, M.H., Zhang, L.i., Kremer, D., Hwang, R.F., Witkiewicz, A.K., Ying, H., Asara, J.M., Evans, R.M., Cantley, L.C., Lyssiotis, C.A., Kimmelman, A.C., 2016. Pancreatic stellate cells support tumour metabolism through autophagic alanine secretion. Nature 536 (7617), 479–483.
Stegemeier, J.P., Schwab, F., Colman, B.P., Webb, S.M., Newville, M., Lanzirotti, A., Winkler, C., Wiesner, M.R., Lowry, G.V., 2015. Speciation matters: bioavailability of silver and silver sulfide nanoparticles to Alfalfa (*Medicago sativa*). Environ. Sci. Technol. 49 (14), 8451–8460.
Toader-Williams, A., Golubkina, N., 2009. Investigation upon the edible snail's potential as source of selenium for human health and nutrition observing its food chemical contaminant risk factor with heavy metals. Bull. UASVM Agric. 2 (66), 495–499.
UN (United Nations), 2015. Transforming our world: The 2030 534 agenda for sustainable development. https://sdgs.un.org/2030agenda.
USEPA (United State Environment Protection Agency), 2011. Exposure Factors Handbook (2011 Edition). https://www.epa.gov/sites/default/files/2015-09/documents/efh-frontmatter.pdf.
Wang, X., Sun, W., Zhang, S., Sharifan, H., Ma, X., 2018. Elucidating the effects of cerium oxide nanoparticles and zinc oxide nanoparticles on arsenic uptake and speciation in rice (*Oryza sativa*) in a hydroponic system. Environ. Sci. Technol. 52 (17), 10040–10047.
Wang, Z., Yue, L., Dhankher, O.P., Xing, B., 2020. Nano-enabled improvements of growth and nutritional quality in food plants driven by rhizosphere processes. Environ. Int. 142, 105831–105843.
White, J.C., Gardea-Torresdey, J., 2018. Achieving food security through the very small. Nat. Nanotechnol. 13 (8), 627–629.
Wu, F., 2007. Measuring the economic impacts of Fusarium toxins in animal feeds. Anim. Feed Sci. Technol. 137 (3-4), 363–374.
Wu, J., Bosker, T., Vijver, M.G., Peijnenburg, W.J.G.M., 2021. Trophic transfer and toxicity of (mixtures of) Ag and TiO_2 nanoparticles in the lettuce-terrestrial snail food chain. Environ. Sci. Technol. 55 (24), 16563–16572.
Yan, N., Wang, W.-X., 2021. Novel imaging of silver nanoparticle uptake by a unicellular alga and trophic transfer to *Daphnia magna*. Environ. Sci. Technol. 55 (8), 5143–5151.